Available online at www.sciencedirect.com
SCIENCE DIRECT®
Journal of Steroid Biochemistry & Molecular Biology 89–90 (2004) 167–171
The Journal of Steroid Biochemistry & Molecular Biology
www.elsevier.com/locate/jsbmb

Homology modeling of human 25-hydroxyvitamin D_3 1α-hydroxylase (CYP27B1) based on the crystal structure of rabbit CYP2C5☆

Keiko Yamamoto [a,*], Hiroyuki Masuno [a], Natsumi Sawada [b], Toshiyuki Sakaki [b], Kuniyo Inouye [b], Masaji Ishiguro [c], Sachiko Yamada [a,1]

[a] *Institute of Biomaterials and Bioengineering, Tokyo Medical and Dental University, 2-3-10 Kanda-Surugadai, Chiyoda-ku, Tokyo 101-0062, Japan*
[b] *Graduate School of Agriculture, Kyoto University, Sakyo-ku, Kyoto 606-8502, Japan*
[c] *Suntory Institute for Bioorganic Research (SUNBOR), 1-1 Wakayamadai, Shimamoto, Osaka 618-8503, Japan*

Abstract

Seventeen missense mutations of 25-hydroxyvitamin D_3 1α-hydroxylase (CYP27B1) that cause Vitamin D-dependent rickets type I (VDDR-I) have been identified. To understand the mechanism by which each mutation disrupts 1α-hydroxylase activity and to visualize the substrate-binding site, we performed the homology modeling of CYP27B1. The three-dimensional (3D) structure of CYP27B1 was modeled on the basis of the crystal structure of rabbit CYP2C5, the first solved X-ray structure of a eukaryotic CYP. The 3D structure of CYP27B1 contains 17 helices and 6 β-strands, and the overall structural folding is similar to the available structures of soluble CYPs as well as to the template CYP2C5. Mapping of the residues responsible for VDDR-I has provided much information concerning the function of each mutant. We have previously reported site-directed mutagenesis studies on several mutants of CYP27B1 causing VDDR-1, and suggested the role of each residue. All these suggestions are in good agreement with our 3D-model of CYP27B1. Furthermore, this model enabled us to predict the function of the other mutation residues responsible for VDDR-I.

Keywords: 25-Hydroxyvitamin D_3 1α-hydroxylase; CYP27B1; Vitamin D-dependent rickets type I (VDDR-I); Missense mutation; Homology modeling; Three-dimensional (3D) structure; Vitamin D_3; Cytochrome P450

1. Introduction

The hormonally active form of Vitamin D_3, 1,25-dihydroxyvitamin D_3 [1,25-$(OH)_2D_3$], is produced by two separate hydroxylations; first, in the liver at the 25-position and then, in the kidney at the 1α-position [1]. 1,25-$(OH)_2D_3$ directs cellular processes associated with calcium transport, cellular differentiation and growth, and the immune response [2]. 1,25-$(OH)_2D_3$ is catabolized via side-chain hydroxylation at the C-23, -24 or -26 positions followed by various side-chain oxidations [2]. All these oxidation reactions are mediated by three hydroxylase enzymes, vitamin D_3 25-hydroxylase (CYP27A1), 25-hydroxyvitamin D_3 1α-hydroxylase (CYP27B1), and 25-hydroxyvitamin D_3 24-hydroxylase (CYP24), which belong to the cytochrome P450 (CYP) superfamily. These three enzymes are typical mitochondrial (class I) CYPs. There are only six known eukaryotic members of this class of enzyme, three of which are related to Vitamin D metabolism and the other three of which, CYP11A1 [3], CYP11B1, and CYP11B2 [4], are related to steroid oxidations. CYP27B1, which specifically catalyzes hydroxylation at the 1α-position of 25-OHD_3, was ultimately cloned in 1997 in spite of its low expression level and lability [5–8]. Cloning of CYP27B1 confirmed that defects in the enzyme cause vitamin D-dependent rickets type I (VDDR-I), which is manifested by symptoms of hypotonia, weakness, and growth failure, occasionally accompanied by seizures [9]. Up to now, 17 one-point mutants and several frameshift mutants have been reported [10,11], and for a number of these mutants sequence alignment and biochemical studies have suggested reasons for the lack of 1α-hydroxylation activity [12–14].

So far, crystal structures of six prokaryotic CYPs and one eukaryotic CYP have been reported [15–21]. Prokaryotic CYPs are soluble enzymes, whereas eukaryotic CYPs are membrane bound insoluble proteins. The crystal structures

☆ Presented at the 12th Workshop on Vitamin D (Maastricht, The Netherlands, 6–10 July 2003).

* Corresponding author. fax: +81-3-5280-8005.
E-mail addresses: yamamoto.mr@tmd.ac.jp (K. Yamamoto), yamada.mr@tmd.ac.jp (S. Yamada).
[1] Co-corresponding author.

0960-0760/$ – see front matter © 2004 Elsevier Ltd. All rights reserved.
doi:10.1016/j.jsbmb.2004.03.098

of the six prokaryotic CYPs [15–20] indicate that they all adopt similar structural folding, in spite of frequently having less than 20% sequence identity and having vastly different substrate specificity. In 2000, the crystal structure of rabbit CYP2C5 was reported as the first solved X-ray structure of a eukaryotic CYP, revealing that eukaryotic CYP and prokaryotic CYPs share similar structural folding [21]. This prompted us to construct the 3D structure of CYP27B1 by the homology modeling technique using the structure of CYP2C5 as a template, in order to study the mechanism by which each mutation disrupts 1α-hydroxylase activity and to visualize the substrate-binding pocket. In this paper, we report the overall 3D-model structure of CYP27B1 and derive from the constructed 3D-model the function of each residue responsible for VDDR-I.

2. Methods

2.1. Sequence alignment

We aligned the three human CYPs responsible for vitamin D metabolism (CYP27A1, CYP27B1, CYP24) and rabbit CYP2C5 by using ClustalW interfaced with Clustal X (ver. 1.81) for Windows. A part of the computationally derived alignment, namely the D helix including the N- and C-terminal regions of CYP2C5, was modified manually to align D164 of CYP27B1 with an acidic residue of CYP2C5 because D164 has been reported to be important for protein folding [14].

2.2. Modeling

According to the alignment, we constructed a 3D-model of CYP27B1 by using SYBYL modeling software, COMPOSER (Tripos Inc.), and the atomic coordinates of the crystal structure of rabbit CYP2C5 as the template [21]. (1) The backbone of the structurally conserved regions (SCR) (all helices and β-strands, loops having the same number of amino acid residues except the F–G loop, and residues except a few residues adjacent to the insertion or deletion part) was constructed. (2) Backbone structures of the residual parts were constructed with the loop search command of SYBYL and the selected loops were joined to the SCR parts. (3) Side-chains and then, hydrogens were added to the backbone. (4) Heme was merged into the protein as it adopts the same spatial location as the heme of the template CYP2C5. (5) Energy minimization of the constructed structure was performed until energy gradient is lower than 0.1 kcal/(mol Å) on the Tripos force field.

3. Results and discussion

3.1. Sequence alignment and homology modeling

We constructed the 3D structure of CYP27B1 using the crystal structure of CYP2C5 as a template. CYP2C5 is a member of the mammalian microsomal P450 subfamily 2C and selectively hydroxylates the 21-methyl group of progesterone. Sequence alignment was performed as described in Section 2, and the results are shown in Fig. 1. Sequence identity between CYP2C5 and CYP27B1 is 23.5%. Highly conserved and functionally important residues in the CYP superfamily are: (1) three absolutely conserved residues, ExxR in the K helix and C just before the L helix (for example E376, R379, and C455 in CYP27B1); (2) the consensus sequence (A/G)G*x*(E/D)T in the center of the I helix; (3) the consensus sequence F(G/S)*x*G*x*(H/R)*x*C*x*G*xx*(I/L/F)A containing the Cys (C455 in CYP27B1) responsible for

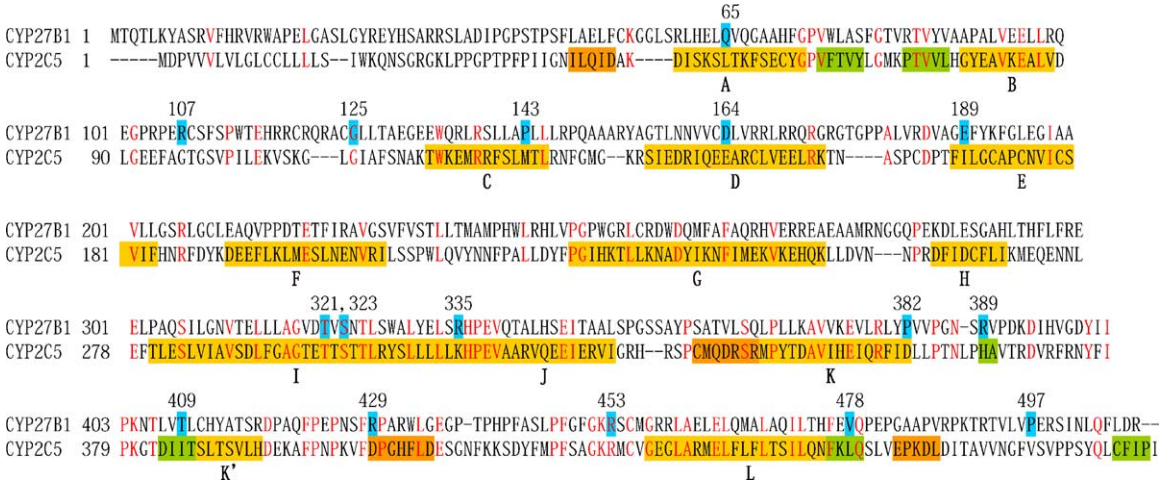

Fig. 1. Sequence alignment of human CYP27B1 with rabbit CYP2C5. The A–L helices are labeled as defined by Williams et al. [21] and are noted below the sequence of CYP2C5. Yellow, orange, and green boxes on CYP2C5 represent α-helix, 3/10 helix, and β-strand, respectively, in the crystal structure of CYP2C5. Blue boxes and the above numbers show residues where point mutation causes VDDR-I. Identical residues in both CYPs are depicted by red letters. (For interpretation of the references to colour in this figure legend, the reader is referred to the web version of the article.)

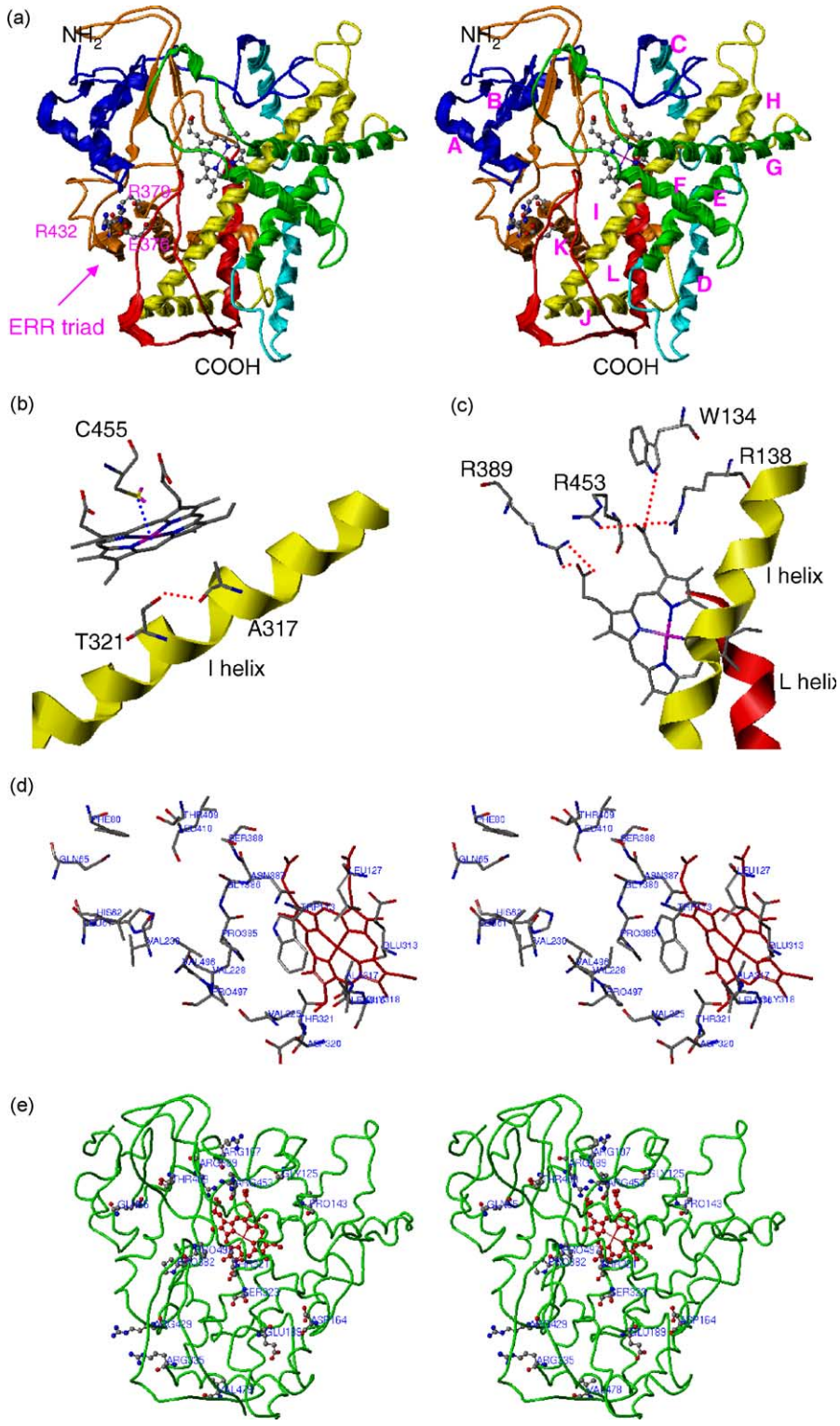

Fig. 2. 3D structure model of CYP27B1. (a) Ribbon loop presentation of CYP27B1 constructed by homology modeling (stereoview). Heme is shown as ball and stick. The ERR triad is shown at the bottom of the left side. (b) C455 as the fifth ligand of Fe of the heme and A317 and T321 on the I helix. (c) Hydrogen bonds between the heme-propionate and highly conserved amino acid residues (W134, R138, R453, and R389). (d) Heme and amino acid residues constituting the substrate binding pocket (stereoview). Heme is depicted in red. (e) Mapping of 17 residues where point mutation causes VDDR-I onto the 3D-model of CYP27B1 (stereoview). Heme is depicted in red.

heme binding [22]. As shown in Fig. 1, these important sequences of both CYPs are correctly aligned with each other. In addition, the residues corresponding to the secondary structure of the crystal CYP2C5 do not have any gaps or insertions (Fig. 1). These show that almost all secondary structure is conserved.

The 3D structure model of CYP27B1 was constructed as described in the Section 2 and is shown in Fig. 2a. The transient N-terminal region and the following region of CYP27B1 (Met1–Ala38) were not constructed because the coordinates of the corresponding region of CYP2C5 were not determined. The F–G loop is assumed to be a substrate-accessible part and is known to be the most flexible region in CYPs. The coordinates of the F–G loop in the template CYP2C5 are lacking. We tentatively constructed this loop based on the topology of P450Bm3, whose F–G loop has the highest similarity to that of CYP27B1 [18]. We evaluated the model structure by using the PROCHECK program. A Ramachandran plot shows that 98.5% of the residues are either in the most favored or allowed regions.

The 3D structure of CYP27B1 was similar to those of other CYPs reported so far. It contains 17 helices (13 α-helices and four 3/10 helices) and 6 β-strands, as does the template CYP2C5. In our model of CYP27B1, E376, R379, and R432 form the ERR triad that is proposed to form the conserved core folding in mitochondrial CYPs [23]. In this ERR triad, E376 forms salt bridge with both R379 (3.0 Å) and R432 (2.9 Å) (Fig. 2a).

The heme is sandwiched between the L helix including its N-terminal loop and the I helix. The sulfide of C455 provides the axial ligand at the fifth coordination site of the heme iron (Fig. 2b). This architecture is responsible for the characteristic absorption spectrum of CYPs, an absorption band with a 450 nm maximum upon binding CO. The propionate side-chain of the D ring of the heme forms hydrogen bonds with R453 before the L helix, and with W134 and R138 located at the N-terminal end of the C helix (Fig. 2c). These three residues are all highly conserved across mammalian CYPs (Fig. 1). The propionate side-chain of the A ring of the heme interacts with R389 in a β-strand (Fig. 2c).

A317 and T321 in the I helix are highly conserved, of which T321 forms a hydrogen bond with the backbone carbonyl oxygen of A317 (Fig. 2b). T321, which is located near the heme, is thought to be involved in the oxygen activation mechanism. Residues whose side-chain faces the substrate-binding pocket are L61, H62, Q65, F80, W113, L127, V225, V228, L316, A317, T321, P385, G386, N387, S388, T409, V496, and P497 (Fig. 2d). This pocket is hydrophobic except for the site surrounded by the A helix and the neighboring four β-strands. The majority of the residues facing the substrate-binding pocket are located in five of six SRSs (substrate recognition sites) proposed by Gotoh [24] excluding SRS3. Thus, our model is successful in explaining the overall 3D structure of CYP27B1.

3.2. Function presumed from 3D-model

The residues where missense mutation causes VDDR-I are shown on the model structure of CYP27B1 (Fig. 2e). We previously reported a mutagenesis study on several mutants of CYP27B1 that cause VDDR-1, and suggested the role of each residue: (1) R107, G125, and P497 have roles in proper folding of the protein; (2) R389 and R453 are involved in heme-propionate binding; (3) D164 stabilizes the 4-helix bundle consisting of the D, E, I, and J helices; (4) R335P disrupts the kink between the I helix and the J helix; (5) T321 is responsible for the activation of molecular oxygen [14]. All these suggestions are in good agreement with our 3D-model of CYP27B1 (Fig. 2). Furthermore, mapping of the residues responsible for VDDR-I on the 3D-model of CYP27B1 provided us with numerous insights with regard to the function of the remaining mutants. From the location of the residues, we infer the following functions for each residue (Table 1). (1) Q65 and/or T409 might bind with the hydroxyl group of 25-OHD_3. These two residues are not conserved among mitochondrial CYPs [14], indicating that they are associated with the specific functions of CYP27B1. (2) Proline has a role as helix breaker. P143L and P382S disrupt this function, whereas R429P breaks the original 3/10 helix, as does R335P. (3) E189, S323, and V478 play an important role in protein folding because the side-chains of these 3 residues are buried inside the protein structure.

In conclusion, we constructed the 3D structure of CYP27B1 which catalyzes the most important hydroxylation in vitamin D metabolism. The 3D structure provided an opportunity to understand the spatial location and function of the residues responsible for mutations with a clinical phenotype. To confirm the function of residues such as Q65, P143, E189, S323, P382, T409, R429, and V478, we are now undertaking experimental studies using a co-expression system of CYP27B1 and chaperonin.

Table 1
Function of residues responsible for VDDR-I

Mutation	Location	Function
Q65H	A helix	H-bond with substrate[a]
R107H	Loop B–C	Folding
G125E	Loop B–C	Folding
P143L	C helix (terminal)	Folding (helix breaker)[a]
D164L	D helix	Folding (4-helix bundling)
E189L	E helix	Folding[a]
T321R	I helix	Oxygen activation
S323Y	I helix	Folding[a]
R335P	I helix	Folding
P382S	K helix (terminal)	Folding (helix breaker)[a]
R389C(H)	β-strand	Heme-propionate binding
T409I	β-strand	H-bond with substrate[a]
R429P	3/10 Helix	Folding[a]
R453C	Loop K'–L	Heme-propionate binding
V478G	β-strand	Folding[a]
P497R	Terminal loop	Folding

[a] Function inferred from the 3D-model of CYP27B1.

References

[1] D.E. Lawson, D.R. Fraser, E. Kodicek, H.R. Morris, D.H. Williams, Identification of 1,25-Dihydroxycholecalciferol, a new kidney hormone controlling calcium metabolism, Nature 230 (1971) 228–230.

[2] D. Feldman, F.H. Glorieux, J.W. Pike (Eds.), Vitamin D., Academic Press, San Diego, 1997.

[3] B.C. Chung, K.J. Matteson, R. Voutilainen, T.K. Mohandas, W.L. Miller, Human cholesterol side-chain cleavage enzyme, P450scc: cDNA cloning, assignment of the gene to chromosome 15, and expression in the placenta, Proc. Natl. Acad. Sci. U.S.A. 83 (1986) 8962–8966.

[4] E. Mornet, J. Dupont, A. Vitek, P.C. White, Characterization of two genes encoding human steroid 11β-hydroxylase (P-450(11)β), J. Biol. Chem. 264 (1989) 20961–20967.

[5] G.K. Fu, D. Lin, M.Y.H. Zhang, D.D. Bikle, C.H.L. Shackleton, W.L. Miller, A.A. Portale, Cloning of human 25-hydroxyvitamin D 1α-hydroxylase and mutations causing vitamin D-dependent rickets type I, Mol. Endocrinol. 11 (1997) 1961–1970.

[6] K. Takeyama, S. Kitanaka, T. Sato, M. Kobori, J. Yanagisawa, S. Kato, 25-Hydroxyvitamin D_3 1α-hydroxylase and vitamin D synthesis, Science 277 (1997) 1827–1830.

[7] T. Shinki, H. Shimada, S. Wakino, H. Anazawa, M. Hayashi, T. Saruta, H.F. DeLuca, T. Suda, Cloning and expression of rat 25-hydroxyvitamin D_3-1α-hydroxylase cDNA, Proc. Natl. Acad. Sci. U.S.A. 94 (1997) 12920–12925.

[8] R. St-Arnaud, S. Messerlian, J.M. Moir, J.L. Omdahl, F.H. Glorieux, The 25-hydroxyvitamin D 1-α-hydroxylase gene maps to the pseudovitamin D-deficiency rickets (PDDR) disease locus, J. Bone Miner. Res. 12 (1997) 1552–1559.

[9] S. Balsan, Hereditary Pseudo-Deficiency Rickets or Vitamin dependency Type I in Rickets, in: F.H. Glorieux (Ed.), Raven Press, New York, 1991, pp. 155–163.

[10] A.A. Portale, W.L. Miller, Human 25-hydroxyvitamin D-1α-hydroxylase: cloning, mutations, and gene expression, Pediatr. Nephrol. 14 (2000) 620–625.

[11] S. Kitanaka, A. Murayama, T. Sakaki, K. Inouye, Y. Seino, S. Fukumoto, M. Shima, S. Yukizane, M. Takayanagi, H. Niimi, K. Takeyama, S. Kato, No enzyme activity of 25-hydroxyvitamin D_3 1α-hydroxylase gene product in pseudovitamin D deficiency rickets, including that with mild clinical manifestation, J. Clin. Endocrinol. Metab. 84 (1999) 4111–4117.

[12] J.T. Wang, C.J. Lin, S.M. Burridge, G.K. Fu, M. Labuda, A.A. Portale, W.L. Miller, Genetics of vitamin D 1α-hydroxylase deficiency in 17 families, Am. J. Hum. Genet. 63 (1998) 1694–1702.

[13] J.L. Omdahl, E.A. Bobrovnikova, S. Choe, P.P. Dwivedi, B.K. May, Overview of regulatory cytochrome P450 enzymes of vitamin D pathway, Steroids 66 (2001) 381–389.

[14] N. Sawada, T. Sakaki, S. Kitanaka, S. Kato, K. Inouye, Structure–function analysis of CYP27B1 and CYP27A1. Studies on mutants from patients with vitamin D-dependent rickets type I (VDDR-I) and cerebrotendinous xanthomatosis (CTX), Eur. J. Biochem. 268 (2001) 6607–6615.

[15] T.L. Poulos, B.C. Finzel, A.J. Howard, High-resolution crystal structure of cytochrome P450cam, J. Mol. Biol. 195 (1987) 687–700.

[16] C.A. Hasemann, K.G. Ravichandran, J.A. Peterson, J. Deisenhofer, Crystal structure and refinement of cytochrome P450terp at 2.3 Å resolution, J. Mol. Biol. 236 (1994) 1169–1185.

[17] J.R. Cupp-Vickery, T.L. Poulos, Structure of cytochrome P450eryF involved in erythromycin biosynthesis, Nat. Struct. Biol. 2 (1995) 144–153.

[18] K.G. Ravichandran, S.S. Boddupalli, C.A. Hasermann, J.A. Peterson, J. Deisenhofer, Crystal structure of hemoprotein domain of P450BM-3, a prototype for microsomal P450's, Science 261 (1993) 731–736.

[19] L.M. Podust, T.L. Poulos, M.R. Waterman, Crystal structure of cytochrome P450 14α-sterol demethylase (Cyp51) from mycobacterium tuberculosis in complex with azole inhibitors, Proc. Natl. Acad. Sci. U.S.A. 98 (2001) 3068–3073.

[20] S.Y. Park, H. Shimizu, S. Adachi, A. Nakagawa, I. Tanaka, K. Nakahara, H. Shoun, E. Obayashi, H. Nakamura, T. Iizuka, Y. Shiro, Crystal structure of nitric oxide reductase from denitrifying fungus *Fusarium oxysporum*, Nat. Struct. Biol. 4 (1997) 827–832.

[21] P.A. Williams, J. Cosme, V. Sridhar, E.F. Johnson, D.E. McRee, Mammalian microsomal cytochrome P450 monooxygenase: structural adaptations for membrane binding and functional diversity, Mol. Cell 5 (2000) 121–131.

[22] S.E. Graham-Lorence, J.A. Peterson, Structural alignments of P450s and extrapolations to the unknown, Methods Enzymol. 272 (1996) 315–326.

[23] I.A. Pikuleva, C. Cao, M.R. Waterman, An additional electrostatic interaction between adrenodoxin and P450c27 (CYP27A1) results in righter binding than between adrenodoxin and P450scc (CYP11A1), J. Biol. Chem. 274 (1999) 2045–2052.

[24] O. Gotoh, Substrate recognition site in cytochrome P450 family 2 (CYP2) protein inferred from comparative analyses of amino acid coding nucleotide sequences, J. Biol. Chem. 267 (1992) 83–90.